energies

MDPI

Article

Detailed Analysis of the Effects of Biodiesel Fraction Increase on the Combustion Stability and Characteristics of a Reactivity-Controlled Compression Ignition Diesel-Biodiesel/Natural Gas Engine

Mohammad Taghi Zarrinkolah [1] and Vahid Hosseini [2,*]

[1] School of Mechanical Engineering, Sharif University of Technology, Azadi Ave, Tehran 1458889694, Iran; zarrinkolah_mt@mech.sharif.edu
[2] School of Sustainable Energy Engineering, Faculty of Applied Sciences, Simon Fraser University, 10285 University Drive, Surrey, BC V3T 0N1, Canada
* Correspondence: v_hosseini@sfu.ca

Abstract: A single-cylinder marine diesel engine was modified to be operated in reactivity controlled compression ignition (RCCI) combustion mode. The engine fueling system was upgraded to a common rail fuel injection system. Natural gas (NG) was used as port fuel injection, and a diesel/sunflower methyl ester biodiesel mixture was used for direct fuel injection. The fraction of biodiesel in the direct fuel injection was changed from 0% (B0; 0% biodiesel and 100% diesel) to 5% (B5) and 20% (B20) while keeping the total energy input into the engine constant. The objective was to understand the impacts of the increased biodiesel fraction on the combustion characteristics and stability, emissions, and knocking/misfiring behavior, keeping all other influential parameters constant. The results showed that nitrogen oxides (NOx) emissions of B5 and B20 without the need for any after-treatment devices were lower than the NOx emission limit of the Euro VI stationary engine regulation. B5 and B20 NOx emissions decreased by more than 70% compared to the baseline. Significantly more unburned hydrocarbons (UHCs) and carbon monoxide (CO) emissions were produced when biodiesel was used in the direct fuel injection (DFI). The results also showed that using B5 and B20 instead of B0 led to an increase of 18% and 13.5% in UHCs and an increase of 88.5% and 97% in CO emissions, respectively. Increasing the biodiesel fraction to B5 and B20 reduced the maximum in-cylinder pressure by 3% and 10.2%, respectively, compared to B0. Combustion instability is characterized by the coefficient of variation (COV) of the indicated mean effective pressure (IMEP), which was measured as 4.2% for B5 and 4.8% for B20 compared to 1.8% for B0. Therefore, using B20 and B5 resulted in up to 34.9% combustion instabilities, and 18.5% compared to the baseline case. The tendency for knocking decreased from 13.7% for B0 to 4.3% for B20. The baseline case (B0) had no misfiring cycle. The B5 case had some misfiring cycles, but no knocking cycle was observed. Moreover, the historical cyclic analysis showed more data dispersions when the biodiesel fraction increased in DFI. This study shows the potential of biodiesel replacement in NG/diesel RCCI combustion engines. This study shows that biodiesel can be used to effectively reduce NOx emissions and the knocking intensity of RCCI combustion. However, combustion instability needs to be monitored.

Keywords: reactivity-controlled compression ignition combustion; biodiesel/diesel blends; combustion stability; cyclic variations; nitrogen oxides; carbon monoxide; unburned hydrocarbons; soot

check for updates

Citation: Zarrinkolah, M.T.; Hosseini, V. Detailed Analysis of the Effects of Biodiesel Fraction Increase on the Combustion Stability and Characteristics of a Reactivity-Controlled Compression Ignition Diesel-Biodiesel/Natural Gas Engine. *Energies* **2022**, *15*, 1094. https://doi.org/10.3390/en15031094

Academic Editor: Amin Paykani

Received: 21 December 2021
Accepted: 24 January 2022
Published: 1 February 2022

Publisher's Note: MDPI stays neutral with regard to jurisdictional claims in published maps and institutional affiliations.

Copyright: © 2022 by the authors. Licensee MDPI, Basel, Switzerland. This article is an open access article distributed under the terms and conditions of the Creative Commons Attribution (CC BY) license (https://creativecommons.org/licenses/by/4.0/).

1. Introduction

Fossil fuels are the main culprit of climate change and global warming. Nowadays, many fossil fuels are used in internal combustion engines for transportation and power generation. The depletion of fossil fuels and the harmful pollutants produced by their

consumption are two significant problems that scientists face. Thus, many efforts are being made to make the world independent of fossil fuels, especially in the transportation industry. Using alternative and renewable fuels as substitutes for fossil fuels can be considered as a solution. Various harmful pollutants emitted by fossil fuels also pose a serious threat to human health, which has compelled scientists to discover new ways to reduce them [1].

Diesel engine nitrogen oxides (NOx) and soot emissions adversely affect human health and the environment [2]. NOx is a lung irritant and a precursor to ozone formation [3]. Diesel soot particles are known carcinogens and have been linked to cardiovascular diseases [4]. Soot particles also contribute significantly to global warming [5]. Reactivity-controlled compression ignition (RCCI) combustion as a low-temperature combustion (LTC) strategy has been introduced to enhance the engine's fuel economy while reducing NOx and soot engine-out emissions simultaneously [6–9]. The RCCI combustion mode uses two or more fuels with different reactivity. The low-reactivity fuel is often injected into the engine intake port, and high-reactivity fuel is directly injected into the combustion chamber for combustion phasing control [10]. With the help of the reactivity gradient difference between the two fuels and setting an optimized start for the injection timing, a high-efficiency combustion mode with low NOx and soot emissions is achieved [11–13]. Unlike other LTC strategies, such as homogeneous charge compression ignition (HCCI) combustion [14], and partially premixed charge (PPC) combustion [15], RCCI combustion has the advantage of combustion phasing controllability using fuel reactivity stratification [16,17]. Despite the benefits of the RCCI combustion strategy, there are still some challenging problems related to the use of this type of combustion. RCCI engines have a high ringing intensity under higher loads and high UHCs, and CO emissions under lower loads [18–20].

Biodiesel fuels, as a biofuel type, can be mixed with diesel and used mainly as high-reactivity fuel in RCCI combustion. Compared to diesel, a further reduction in CO_2 emissions is achieved by using biodiesel fuels in RCCI combustion [21]. The benefits also include lower NOx and soot emissions. An increase in the biodiesel fraction leads to a lower global warming effect due to a decrease in the CO_2 emissions produced during the combustion process [22].

Biodiesel/diesel blends are used as a high-reactivity fuel without any significant modifications of the engines. Biodiesel fuels are produced from agricultural products, food waste, cooking oil waste, and many other resources [1,23]. Compared to conventional diesel fuel, biodiesel fuel generates fewer emissions at the same power level. They protect moving engine parts from increased abrasion owing to their high viscosity [24]. Biodiesel fuels are more expensive than diesel fuels, have lower cloud points, and do not atomize well in the combustion chamber due to higher kinematic viscosity [25,26]. Certain amounts of additives, such as n-butanol (10% by volume) and graphene oxide nanoparticles (90 ppm), can improve the properties of Nigella sativa biodiesel and lead to better combustion [27]. In another study, by adding zinc oxide nanoparticles to a Mahua biodiesel/diesel blend, the brake thermal efficiency increased up to 16.4%, NOx emissions decreased by 7.79%, and UHC emissions were reduced by 13.1% [28]. New generations of biodiesels, such as hydro-treated vegetable oil, contribute to a decrease in CO_2 emissions because they are produced in a carbon-neutral way [29]. Biodiesel blended fuels are conventionally named BXX, which indicates the volumetric percentage of biodiesel in the blend. Blends of B20 and lower than that are used in diesel engines without requiring any change in the engine design and control calibration [25]. B20 is the most common biodiesel blend, and B5 is usually used in transportation [30,31].

Biodiesels are rarely used in RCCI combustion engines as port fuel injection [32] and are often used as direct fuel injection [33,34]. Using 7% by volume of biodiesel in diesel fuel as direct fuel injection (DFI) in a single-cylinder Euro VI diesel engine, the indicated thermal efficiency of combustion in the RCCI mode increases up to 2% compared to common diesel combustion under 25% to 35% load conditions [35]. The combustion characteristics and emissions of vegetable biodiesel fuel/hexanol RCCI engine combustion

were investigated in a single-cylinder diesel engine. By varying the biodiesel/hexanol ratio, the optimum fuel ratio was obtained for each injection pressure. In this study, the thermal efficiency slightly increased, but NOx and soot emissions were decreased compared to diesel RCCI combustion [34]. In another biodiesel RCCI study, NOx was reduced by 22% and smoke particles were decreased by 32% by applying an optimized range of 10 to 20% cottonseed biodiesel fuel at the intake manifold [13]. Higher carbon monoxide (CO) and UHC emissions and lower soot emissions were reported when 80% biofuel (n butanol, 2,5-dimethylfuran) was used as PFI rather than pure biodiesel [33]. Due to low temperatures and lean air/fuel mixture, high CO and UHC emissions in RCCI combustion are challenging [36].

Studies were conducted to identify the causes of high UHC and CO [37,38]. Using Pongamia pinata biodiesel and NG/H2 blends, UHC and CO emissions considerably decreased in RCCI combustion. The addition of H2 to compressed natural gas leads to an increase in the flammability range of premixed fuel and an increase in O and OH radical concentrations, which improves the oxidation rate of UHC and CO [39]. In a gasoline and PFI/biodiesel blend DFI RCCI combustion experimental study, increasing the biodiesel fraction from B0 to B20 and B100 reduced the maximum heat release rate and maximum in-cylinder pressure [40]. It was also reported that the fraction of gasoline in PFI increased from 10% up to 50%, and the specific fuel consumption, CO, and UHC increased while NOx was reduced by nearly half. Various safflower biodiesel/diesel blends were prepared to prevent a longer ignition delay [41]. Since the cetane number of safflower biodiesel is greater than diesel, a more reactive direct injection fuel was obtained when the fraction of biodiesel in blended fuel was increased [42]. The instability of RCCI combustion may cause combustion to fluctuate between knocking and misfiring cycles. In a study, the combustion cyclic variations of three LTC strategies, including partially premixed charge (PPC), HCCI, and RCCI combustion at the same indicated mean effective pressure (IMEP) and CA50, were compared. It was concluded that the cyclic variations of CA50 in RCCI combustion are greater than HCCI and PPC [43]. Direct fuel injection phasing characterized by the start of injection (SOI) is an essential influential parameter of cyclic combustion variation. An early SOI results in a higher maximum pressure rise rate and lower combustion stability [44]. SOI phasing close to TDC leads to improved combustion stability [45]. Another study reported that SOI phasing that is too early causes engine misfire [46]. It was also reported that an increase in the NG fraction (as PFI) leads to higher cyclic variation and lower combustion stability. The combustion stability of dual-fuel combustion was investigated by COV_{IMEP} and COV_{Pmax}. The effect of the addition of NG to the intake manifold on the combustion stability and unregulated emissions was experimentally investigated. Increasing the NG fraction of energy and decreasing the engine load increased the combustion instability [47]. In contrast, few recent articles [44,46,48] have addressed the RCCI combustion stability issue, and the effects of parameters, such as exhaust gas recirculation, PFI mass [46,48], SOI timing [44,46], and direct fuel split injection [46], on the combustion stability of RCCI combustion have been studied. Duraisamy et al. [48] investigated the effect of various types of cooled/hot EGR and PFI fraction on the cyclic variations of combustion. They reported that cyclic variations increased by increasing the PFI fraction. More stable combustion was achieved by using 26% cooled EGR compared to no EGR and 40% EGR cases. Maurya et al. [46] studied the effect of the SOI timing of direct fuel on the combustion stability of RCCI engines. By advancing the SOI timing, the COV_{IMEP} increased, and combustion became more unstable. Moreover, they showed that for the same SOI timing, gasoline-diesel RCCI combustion was more stable than methanol-diesel RCCI combustion due to lower cyclic variations.

Combustion stability is an important issue in LTCs that has not been addressed as it should be, and as mentioned above, few pieces of research have been devoted to this subject. No study has investigated the impact of increasing the biodiesel fraction in DFI on RCCI combustion stability. Therefore, the primary purpose of this study was to investigate the feasibility of using sunflower methyl ester biodiesel fuel as an additive to diesel direct

fuel injection in RCCI combustion and its impact on the emissions, behavior, and stability of combustion. The use of biodiesel as a fuel with the potential to reduce greenhouse gas in RCCI combustion engines also benefits reduced NOx and soot emissions. Still, combustion instability could be a limiting factor. The present study continues a previous biodiesel/diesel-NG RCCI combustion study [49], analyzing the experimental results regarding RCCI combustion stability.

2. Experimental Setup

A modified single-cylinder, water-cooled Farymann diesel engine was used for the experiments. The engine specifications are shown in Table 1. A schematic of the test rig is shown in Figure 1, and the piston bowl shape is shown in Figure 2.

Table 1. Farymann 18 W diesel engine specifications.

Parameter	Value
Number of Cylinders	1
Cooling System	Water-cooled
Maximum Power	4.7 kW at 3000 rpm
Maximum Speed (rpm)	3600
Maximum Torque	16.7 Nm at 2400 rpm
Displacement Volume (cm^3)	290
Bore (mm)	82
Stroke (mm)	55
Compression Ratio	18:1

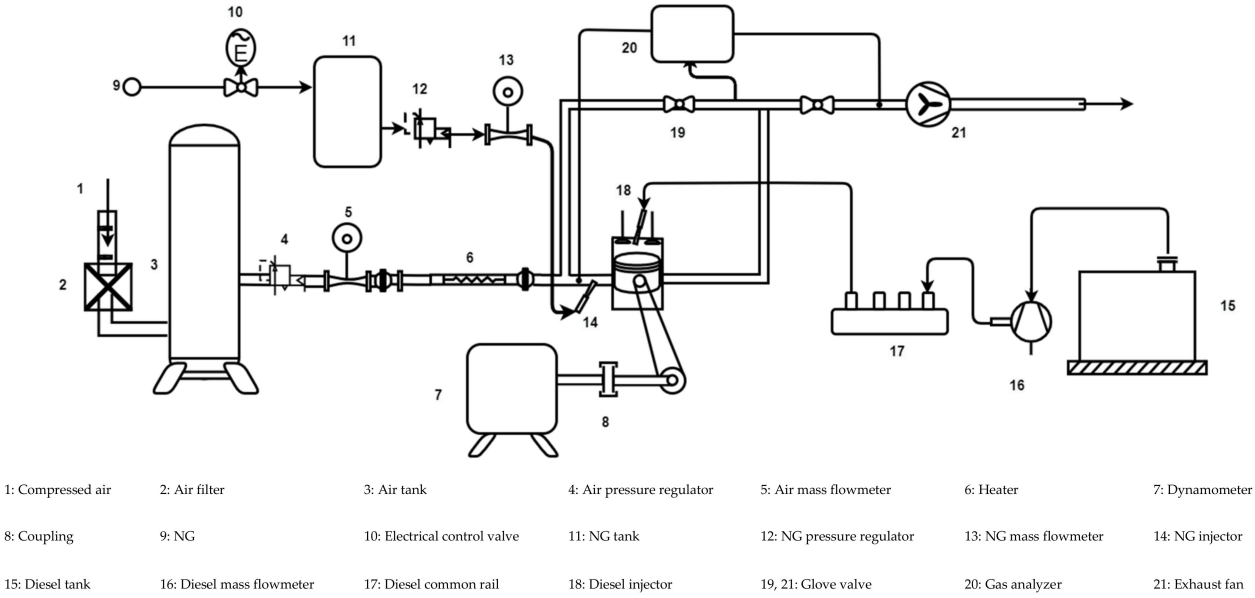

Figure 1. A schematic of the single-cylinder RCCI engine experimental setup.

The PFI system prepares a semi-homogeneous mixture of natural gas and air. The diesel/biodiesel blend is directly injected into the combustion chamber through a direct fuel injector, the specifications of which are given in Table 2.

The cylinder pressure was measured using a water-cooled piezoelectric Kistler model 6043/A60 pressure transducer. Intake airflow was facilitated using a compressor that increased the pressure up to 7 bar and stored it in a surge tank. The intake air pressure was adjusted to the desired value using a pressure regulator. The intake temperature was set to any desired value using two immersion-style heaters and a PID controller. All gaseous emissions were measured using a HORIBA model MEXA-584L five-gas emission analyzer.

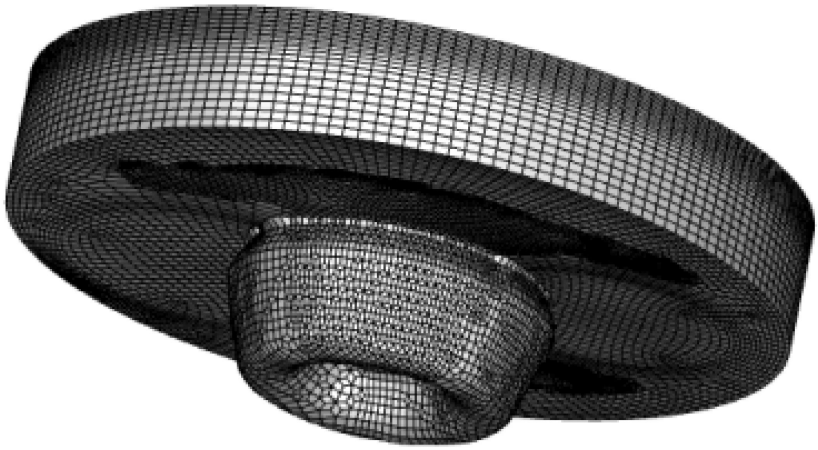

Figure 2. Combustion chamber geometry of a Farymann single-cylinder engine.

Table 2. Common rail injector specifications.

Parameter	Value
Number of holes	8
Hole diameter (μm)	120
Spray Angle (measured vertically)	120
Injection Pressure (bar)	400
Number of injections per cycle	1

3. Experiment Procedure

The experiments were performed at a constant engine speed. NG as PFI and B0 (0% biodiesel and 100% diesel by volume), B5 (5% biodiesel and 95% diesel by volume), and B20 (20% biodiesel and 80% diesel by volume) as DFI were used. Each biodiesel blend was stirred well and left to reach equilibrium in environmental conditions. According to [50], the density, heating value, and kinematic viscosity of blends have a linear relationship with the biodiesel content of blends with lower than 30% biodiesel. Some properties of the diesel, sunflower methyl ester as biodiesel fuel, and NG used in the experiments are given in Table 3.

Table 3. Some properties of the diesel, biodiesel (sunflower methyl ester), and NG fuels [42,51].

Property	Biodiesel	Diesel	NG
Density at 15 °C (kg/m^3)	0.883	0.83	-
Kinematic viscosity (mm^2/s) at 40 °C	4.53	2.3	-
LHV (MJ/kg)	37.75	43.7	48
Cloud point temperature (°C)	2	−35	-
Flash point temperature (°C)	192	128	-
Cetane number (-)	49.5	51	

Direct and port fuel injections were carried out at constant pressures of 400 and 3 bar, respectively. The temperature and gauge pressure of the inlet air was set to 37 °C and 0.4 bar. The cooling water temperature was also set to 60 °C. In all experiments, the total energy input to the engine was kept constant. PFI provided 70% of the total energy input. The rest was provided by DFI of diesel and biodiesel. The lower heating value of DFI was calculated by:

$$LHV_{tot}\left[\frac{MJ}{kg}\right] = \frac{m_{DF} \times LHV_{DF} + m_{NG} \times LHV_{NG}}{m_{DF} + m_{NG}} \quad (1)$$

The combustion efficiency (CE) was calculated by the following equation:

$$CE(\%) = \left[1 - \frac{m_{CO}LHV_{CO} + m_{UHC}LHV_{UHC}}{m_{DIF}LHV_{DIF} + m_{PIF}LHV_{PIF}}\right] \times 100 \quad (2)$$

The SOI timing for B0, B5, and B20 were kept constant at −51 CAD aTDC. The operating conditions of the experimental studies are summarized in Table 4.

Table 4. Engine operating conditions.

#	-
Speed(rpm)	1800
DFI pressure (bar)	400
PFI pressure(bar)	3
PFI energy fraction (%)	70
PFI duration (ms)	4.88
DFI duration (μs)	768 (B0), 770 (B5), and (775)
Volumetric percentage of biodiesel in DFI	0, 5, and 20
Port fuel mass (kg/h)	0.256
Direct fuel mass (kg/h)	0.12(B0), 0.121 (B5), and 0.123 (B20)
Total fuel energy (J/cycle)	325
Inlet air temperature (°C)	37
Inlet air gauge pressure (bar)	0.4
Cooling water temperature (°C)	60
PFI	Natural gas
DFI	Diesel and biodiesel
SOI timing	−51 CAD aTDC

4. Uncertainty Analysis

In each experimental work, there are some sources of error that make the measurement results different from the real values. These measurement errors are generally categorized into bias and random or precision errors. Bias errors are systematic errors related to calibration and are constant over the experimentation. Measurement errors usually arise from a change in the environmental conditions, human-related miscalculations, and errors due to measuring instruments [52]. Therefore, uncertainty analysis of the experimental results as an important tool for the calculation of errors is mandatory. In this study, uncertainty analysis of the emissions was conducted using the method described in [52]. In each operating condition, the experiments were repeated four times and uncertainty was calculated by means of the standard deviation. Uncertainty corresponding to the combustion efficiency, combustion duration, ignition delay, and engine-out emissions was also calculated and is plotted as error bars in Section 5.

5. Results and Discussion

5.1. Engine Performance

Figure 3 shows the median in-cylinder pressure and rate of heat release corresponding to various volume fractions of biodiesel (B0, B5, and B20) over 300 consecutive cycles. The SOI timing is the same for all three fractions, and it is 51 CAD aTDC. As seen in Figure 3, increasing the biodiesel fraction decreased the maximum in-cylinder pressure and heat release rate. Figure 4 shows the impact of the increase in the biodiesel fraction on the combustion efficiency, combustion duration, and ignition delay. According to Figure 4, as the biodiesel fraction increases, the start of combustion is delayed, and combustion occurs further in the expansion stroke. The maximum in-cylinder pressure decreases due to the later combustion. The maximum in-cylinder pressure is reduced by 3% for B5 and 10.2% for B20 compared to B0.

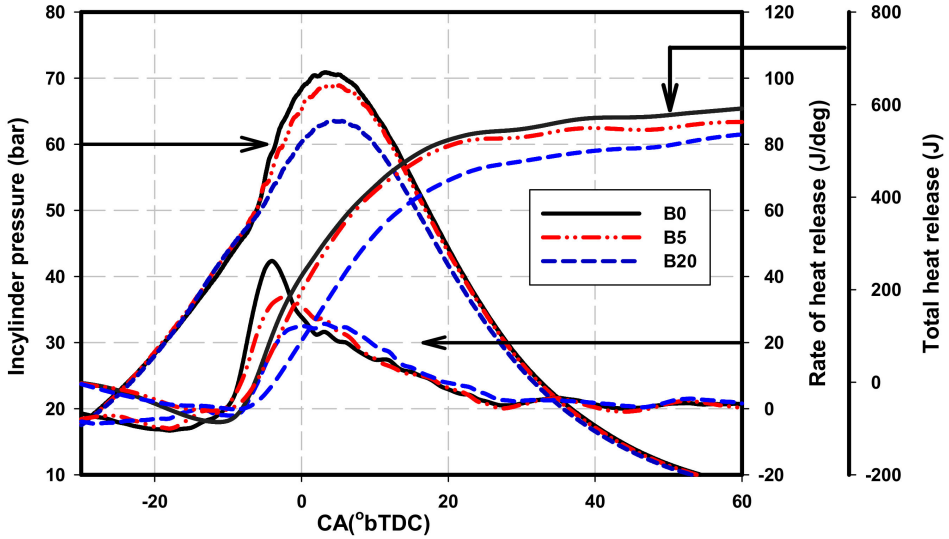

Figure 3. In-cylinder pressure and heat release rate for B0, B5, and B20 at a constant engine speed of 1800 rpm, SOI = −51 CAD aTDC, PFI energy fraction is 70%.

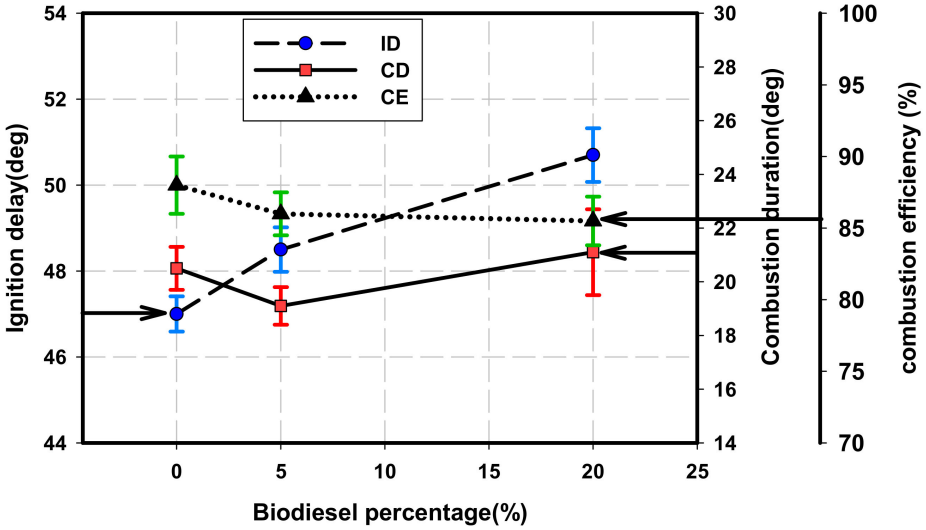

Figure 4. Impact of the increased biodiesel DFI fraction on the ignition delay (ID), combustion duration (CD), and combustion efficiency (CE).

It is common to define the start/end of combustion by the CA10/CA90 (crank angle due to 10/90% of heat release). The combustion duration (CD) is defined as the time interval between CA10 and CA90. The ignition delay (ID) is defined as the time between the start of direct fuel injection and the start of combustion.

The ignition delay changes to biodiesel fractions are shown in Figure 4. The ignition delay increases by increasing the biodiesel share in the biodiesel/diesel blended fuel. The latent heat of vaporization of the biodiesel fuel is higher than that of the diesel fuel at a temperature above 430 K [53]. Moreover, the kinematic viscosity of biodiesel fuel is greater than that of diesel, and as a result, the biodiesel fuel does not atomize well and has larger spray droplet sizes than diesel. Therefore, due to the higher latent heat of vaporization, larger spray droplet sizes, and higher density of biodiesel fuel, a longer ignition delay was observed for B20 and B5 than B0.

As shown in Figure 4, by increasing the biodiesel share, CD decreases and then increases. According to Table 4, in the case of B20, 2.5% more DFI mass is injected into the cylinder compared to B0 and because of this, CD of B20 is slightly more than that of

B0. The combustion efficiency calculated with Equation (2) in the previous section is also shown in Figure 4. According to Figure 4, the total amount of heat released in the B5 and B20 cases is lower than that of B0 and consequently, the maximum in-cylinder temperature decreases. Hence, the lower maximum temperature inside the cylinder leads to incomplete combustion/oxidization of fuels and CE decreases.

5.2. Engine-Out Emissions

The effect of the biodiesel volume fractions in the direct injection blended fuel on NOx, UHC, CO, and CO_2 engine-out emissions is shown in Figure 5. Despite the differences in the experimental procedure of the current study and emission regulation procedures, to obtain an overview of the engine-out emissions produced in the experiments, the NOx, UHC, and CO values were compared with the Euro V and Euro VI emission standard limits for heavy-duty diesel engines under steady-state conditions [54]. It was found that when B5 and B20 were used as DFI, the temperature inside the cylinder—as the most crucial factor in NOx formation—was reduced, and consequently, NOx emissions emitted by the engine were significantly decreased. Compared to B0, NOx emissions decreased by 71.3% and 74.1% when B5 and B20 were applied, respectively. In [55], the authors also reported that the use of B20 instead of neat diesel results in a 58.7% reduction in NOx emissions. The NOx emission values were compared to the NOx limits of the Euro V and Euro VI emissions standards for heavy-duty diesel engines under steady-state conditions. As shown in Figure 5, the NOx values of B5 and B20 are lower than the NOx limit of the Euro VI standard. Therefore, without any exhaust after-treatment device, biodiesel/diesel blends as a fuel composition strategy can be used in RCCI engines to reduce NOx to values below the NOx limit of the Euro VI emissions standard.

UHC production in RCCI combustion engines is typically due to lean fuel regions, low combustion temperatures, and incomplete combustion of the air-fuel mixture inside the cylinder [56]. By increasing the amount of biodiesel in the direct injection blended fuel, the temperature inside the cylinder decreases and the energy source is inadequate for complete oxidization of the premixed charge (NG/air), and as a result, more UHC and CO and lower CO_2 emissions are produced. Moreover, by using B20 instead of B0, 2.5% more DFI mass exists in the combustion chamber, and this is one result of the greater UHC emissions of B20 compared to B0. Using B5 and B20 instead of B0 leads an increase of 18% and 13.5% in UHCs emissions, respectively. A study by Wategave et al. [55] reported that using B20 rather than B0 leads an increase of 77% in CO emissions, while in this study, a 97% increase in CO emissions was observed. The authors of [51] also reported that by replacing B20 instead of B0, UHC emissions increased by 61%. According to Figure 5b,c, the amounts of CO and UHC reported are much greater than the corresponding value of the Euro V/Euro VI standard limits. This is one of the challenges RCCI combustion faces under low- and medium-load conditions [16,57].

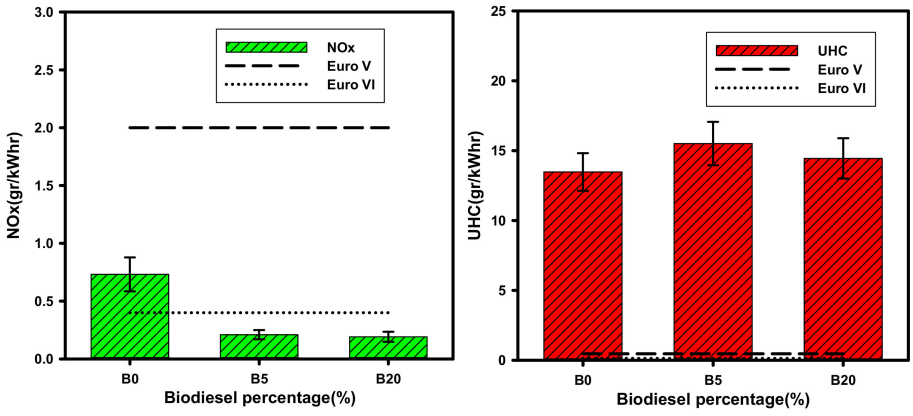

Figure 5. *Cont.*

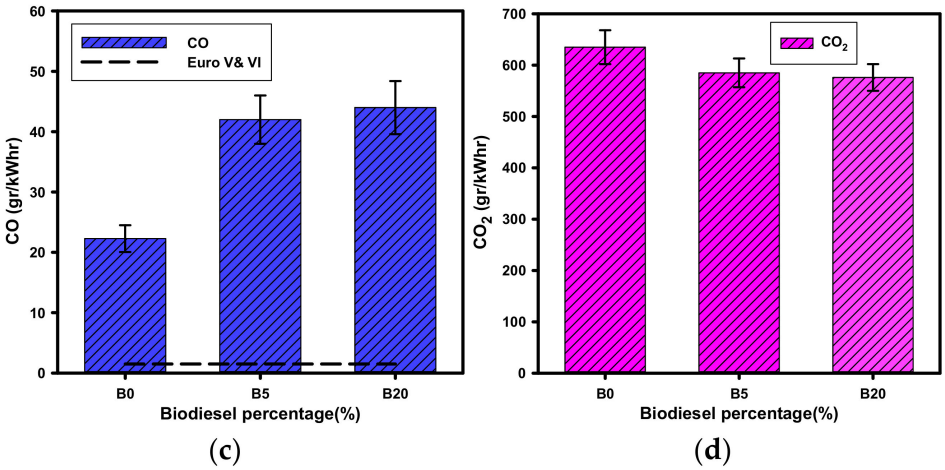

Figure 5. Impact of increasing the biodiesel fraction on engine-out emissions, compared to steady-state stationary diesel engine emission limits of European Euro VI and Euro V: (**a**) NOx engine-out emissions; (**b**) UHC engine-out emissions; (**c**) CO engine-out emissions; (**d**) CO_2 engine-out emissions.

5.3. Combustion Stability

5.3.1. Cyclic Variations in the Combustion Parameters

The time series corresponding to IMEP of 300 consecutive cycles and the IMEP frequency distribution for B0, B5, and B20 are shown in Figure 6. By increasing biodiesel, the standard deviation from the corresponding mean value increases. The IMEP standard deviation increases by 96% and 120% for the B5 and B0 cases in comparison to B0, and this indicates that combustion becomes more unstable when biodiesel is used in direct injection blended fuel. The authors of [55] reported that cyclic variations in the pressure rise rate and combustion noise are increased by using B20 (Karanja biodiesel) instead of B0, but [50] reported that the use of biodiesel (Palm oil) leads to lower cyclic variations. Thus, depending on the physical and chemical properties of the biodiesel used, combustion can be more stable or unstable. The statistical information related to Figure 6 is shown in more detail in Table 5. In statistical studies, the data point that falls outside twice the standard deviations from the mean value on both sides is considered as an outlier. According to Table 5, the percentage of outliers increases from 3% to 7.3% when biodiesel fraction changes from 0 to 20%.

Table 5. IMEP statistics for B0, B5, and B20.

Case #	IMEP < Mean + σ IMEP > Mean − σ		Mean + σ < IMEP < Mean + 2σ Mean − 2σ < IMEP < Mean − σ		IMEP > Mean + 2σ IMEP < Mean − 2σ		IMEP Range	Number of Cycles	%
	Number (of 300 Cycles)	%	Number (of 300 Cycles)	%	Number (of 300 Cycles)	%			
B0	205	68.3	86	28.7	9	3	3.9–4.1	283	94.3
B5	203	67.7	81	27	14	5.3	3.1–3.6	287	95.7
B20	211	70.4	67	22.3	22	7.3	3.1–3.7	288	96

According to Table 5, more than 90% of cycles occur in a narrower IMEP range (3.9–4.1 bar) for B0 and in a wider range for B5 (3.1–3.6 bar), and B20 (3.1–3.7 bar).

The SOC in RCCI combustion is significantly affected by parameters, such as fuel reactivity stratification, local equivalence ratio, temperature gradient, and residual gas remaining in the cylinder from the former engine cycles, which result in variations in SOC [56]. The effect of the addition of biodiesel to diesel on the cyclic variations in SOC and CD for 300 successive cycles was investigated, and the SOC and CD time series corresponding to these consecutive cycles are shown in Figure 7.

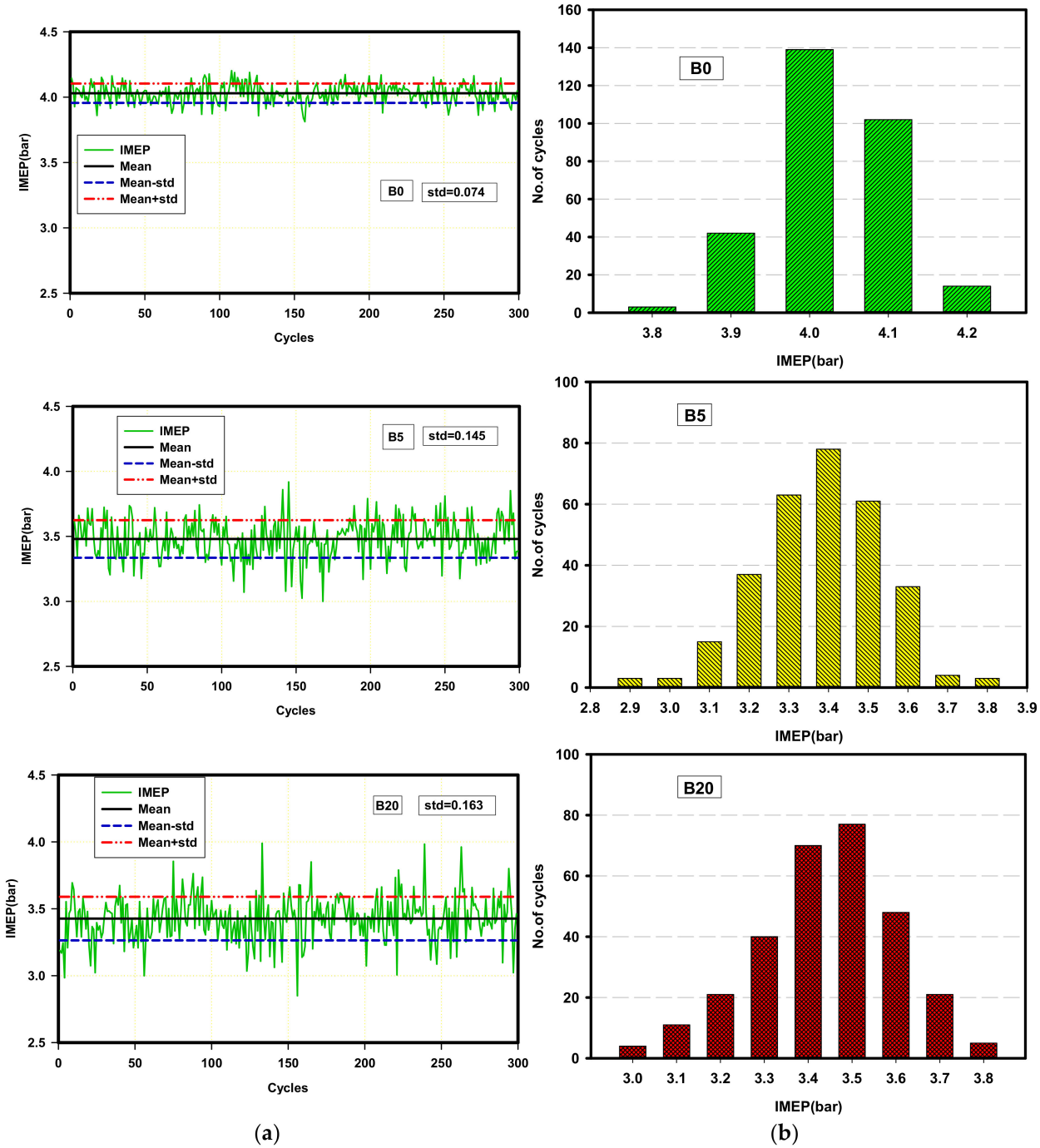

Figure 6. Time series of IMEP: (**a**) for 300 consecutive cycles; (**b**) Frequency distribution of IMEP.

According to Table 5, more than 90% of cycles occur in a narrower IMEP range (3.9–4.1 bar) for B0 and in a wider range for B5 (3.1–3.6 bar) and B20 (3.1–3.7 bar).

It can be found that by increasing the biodiesel fraction, the mean value of SOC and the standard deviation are both increased. The retarded combustion phasing is the main reason for the SOC variations. In some engine cycles of the SOC time series related to B20, there are considerable higher deviations from the SOC mean value and SOC happens too early, which represents incomplete fuel burning in prior cycles. According to Figure 7, irregular CD with high fluctuation amplitudes is seen for B20, and its standard deviation is almost double that of the B0 and B20 cases.

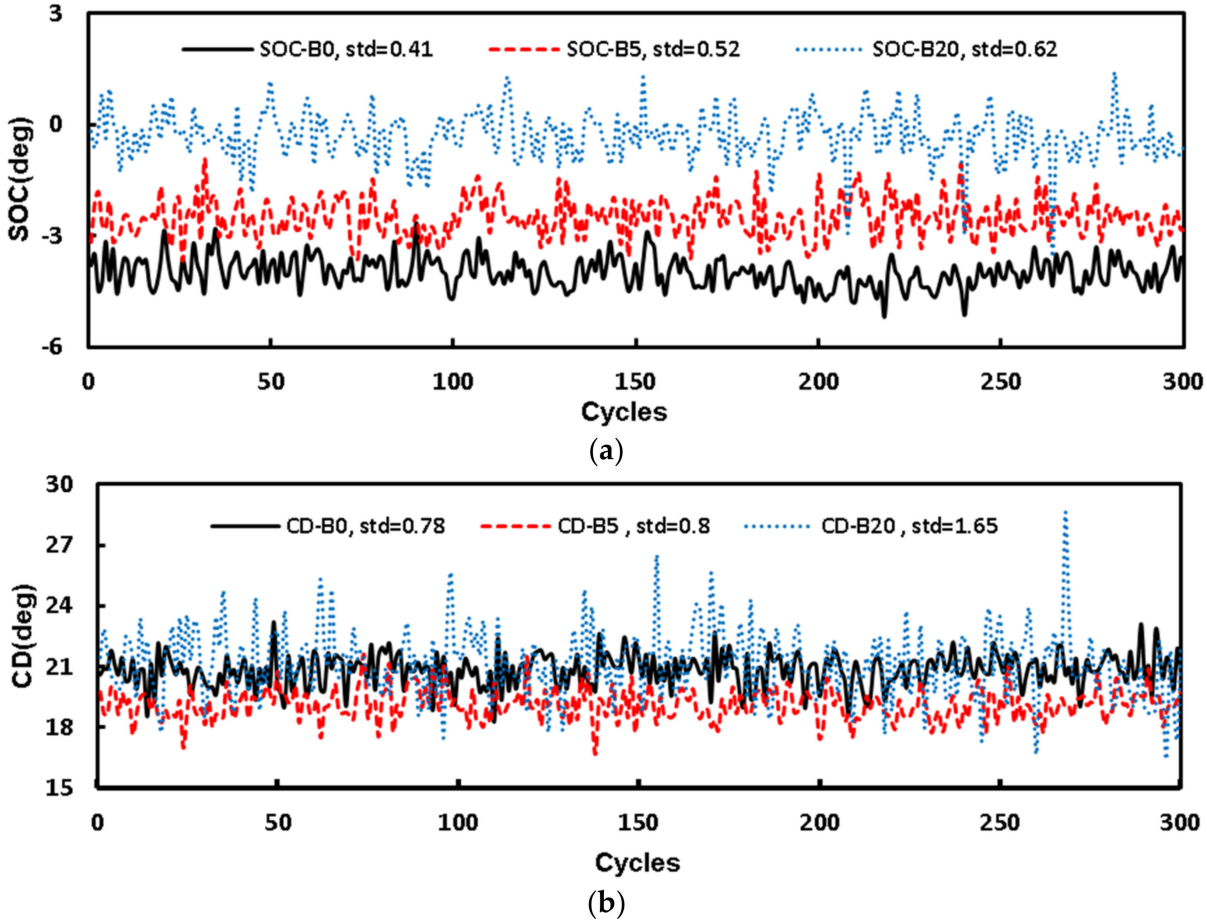

Figure 7. Impact of the increased biodiesel DFI fraction on cyclic variations of combustion parameters: (**a**) SOC variations over 300 consecutive cycles for B0, B5, and B20; (**b**) CD variations over 300 consecutive cycles for B0, B5, and B20.

5.3.2. Misfire and Knocking Analysis

Knocking and misfire are two constraints of internal combustion engines' operation [58]. Knocking happens when sudden, rapid, and spontaneous heat release inside the cylinder occurs [59] and causes high-pressure fluctuations and noisy combustion. On the other hand, misfire as a result of incomplete combustion can also limit the operation of the engine and causes damage to the exhaust after-treatment devices [60].

As shown in Table 6, the knocking propensity of B0 is higher than B5 and B20 because of the lower cetane number of diesel than sunflower biodiesel.

Table 6. Extracted information related to Figure 8.

Case #	$COV_{IMEP} > 5\%$		$R_{max}=\frac{dP}{d\theta}\Big\|_{max} \geq 8\frac{bar}{deg}$	
	Number (of 275 Cycles)	%	Number (of 300 Cycles)	%
B0	0	0	41	13.7
B5	51	18.5	0	0
B20	96	34.9	13	4.3

Misfire or partial burn happens for higher amounts of COV_{IMEP}, and knocking appears at a higher value of $dP/d\theta$. In this study, the conditions $COV_{IMEP} > 5\%$ and $dP/d\theta \geq 8bar/CAD$ are considered as measurements for the misfire and knocking limits, respectively. Figure 8 shows COV_{IMEP} and R_{max} of 275 consecutive combustion cycles

corresponding to B0, B5, and B20. According to Figure 8b, in the case of B0, no misfire combustion cycle was observed, and the variation range of COV_{IMEP} is from 1 to 2.5%. According to Table 6, for the case of B5, 51 combustion cycles of 300 cycles show COV_{IMEP} greater than 5% and thus misfire in 18.5% of the total cycles. By increasing the biodiesel share to 20%, it was found that 34.5% of the total cycles belong to misfire combustion cycles, and COV_{IMEP} varies from 3 to 6.7%.

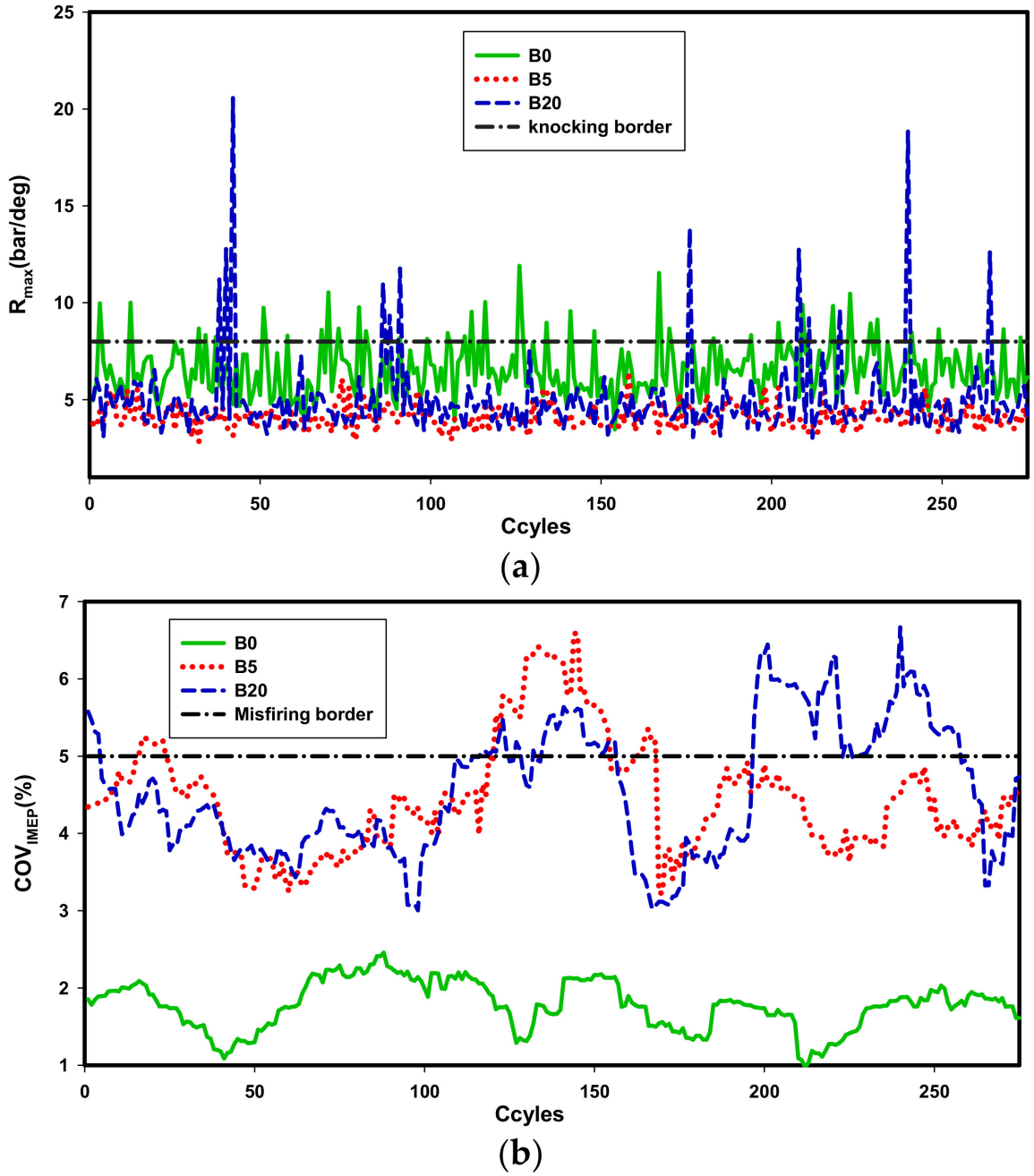

Figure 8. Impact of the increased biodiesel DFI fraction on engine knock and misfire: (**a**) COV_{IMEP} for B0, B5, and B20; (**b**) R_{max} for B0, B5, and B20.

Figure 8a portrays the pressure change rate regarding the crank angle for B0, B5, and B20. In the case of B5, no knocking cycle was observed. It is clearly seen that increasing biodiesel to 5% reduces the tendency to knock, and increasing it to 20% results in fewer but high-intensity knocking cycles in the engine. According to Table 6, the percentage of knocking cycles is 13.7% and 4.3% for B0 and B20, respectively.

5.3.3. Combustion Cyclic Historical Dependency

Using a phase space reconstruction method called return map, the interaction between consecutive cycles of CA10, IMEP, and CD time series was investigated. Return maps of CA10, IMEP, and CD time series data and the relation between each individual pair of cycles are portrayed in Figure 9. The vertical and horizontal axis represents the ith+1 and i^{th} cycle parameter, respectively. These return maps help to additionally comprehend the effect of the addition of biodiesel on the cyclic variations of RCCI combustion and can effectively show the basis of combustion stability [46].

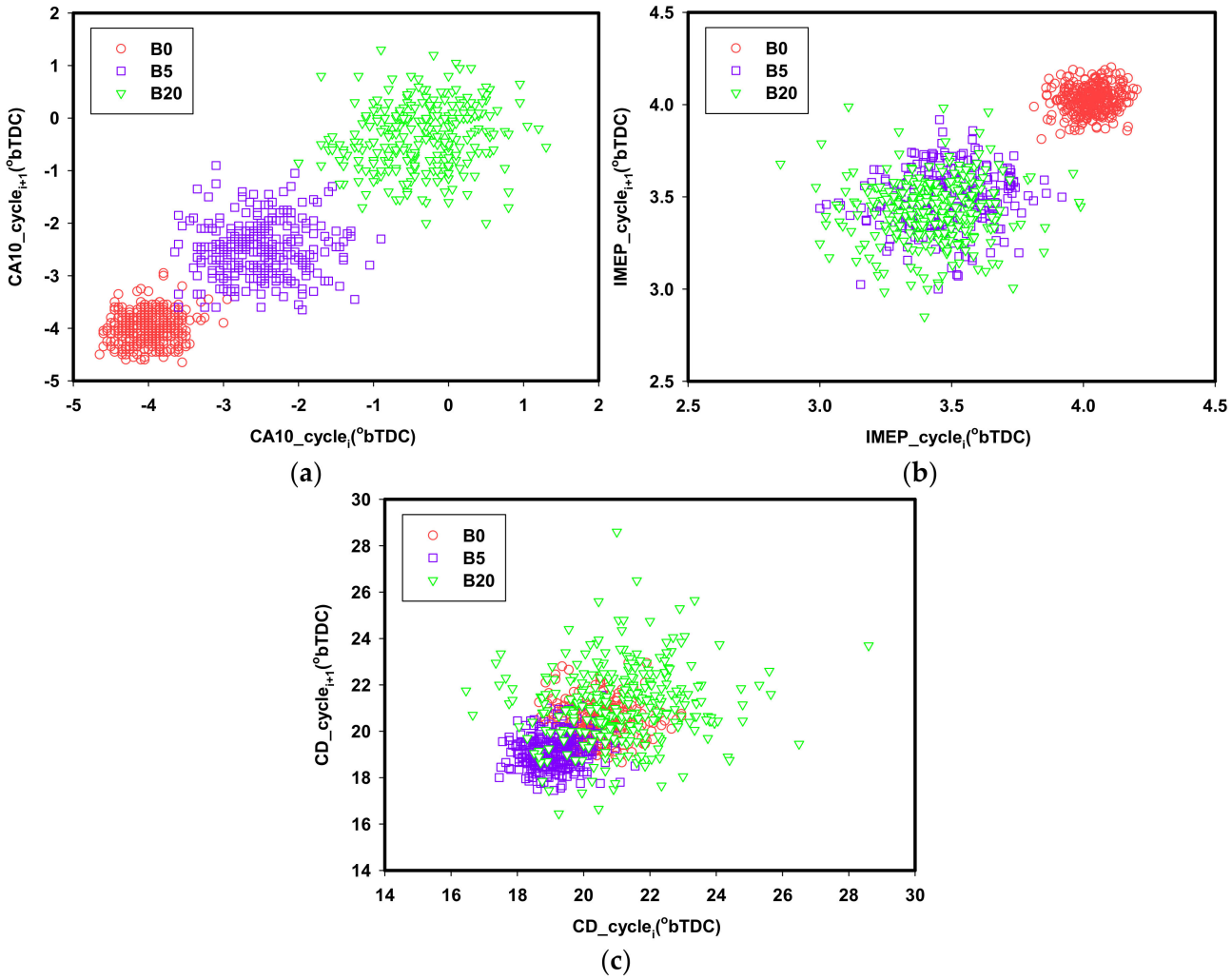

Figure 9. Impact of the increased biodiesel DFI fraction on cyclic historical dependency of combustion parameters: (**a**) Return maps of CA10 time series data for B0, B5, and B20; (**b**) Return maps of IMEP time series data for B0, B5, and B20; (**c**) Return maps of CD time series data for B0, B5, and B20.

According to Figure 9, the time-series data of CA10, IMEP, and CD corresponding to B0 aggregates around its mean value. These slightly dispersed patterns show the stochastic feature of combustion cyclic variations and indicate that no significant correlation exists between successive cycles. As shown in Figure 9, by increasing the amount of biodiesel in DFI, the data dispersion around the corresponding mean values is increased compared to B0. In the B5 and B20 cases, due to misfire and partial burn occurrence in some cycles, the IMEP return map is scattered to lower values. In the B20 case, the return map for CD covers all region of the B0 case, and B5 and is portrayed as an asymmetric shape relative to the 45-degree diagonal line. This indicates some level of correlation related to the previous cycle. In each misfiring cycle, some unburned fuel remains in the combustion chamber and

is burned in the next cycle. Therefore, the next cycle usually has a longer CD and greater energy release. This event has more of an effect on CD rather than IMEP and CA10. So, for the B2O case with the largest number of misfiring cycles, the data dispersion related to CD is relatively greater than IMEP and CA10.

6. Conclusions

An experimental investigation of the changes in the biodiesel fraction in an. NG/diesel RCCI combustion engine was conducted. The objective was to understand the impact of increasing the biodiesel fraction in DFI on engine performance, emissions, stability, knocking/misfiring behavior, and combustion of a single-cylinder research engine. The following were concluded:

1. Increasing the biodiesel fraction from B0 to B5 and B20 reduced NOx emissions by 71.3% and 74.1%, respectively. NOx emissions were reduced to values below the Euro VI limit of a stationary diesel engine with no after-treatment technology;
2. RCCI baseline combustion had high UHCs and CO. Increasing the biodiesel fraction further increased these emissions.
3. Using B5 and B20 instead of B0 led to an increase of 18% and 13.5% in UHCs and an increase of 88.5% and 97% in CO emissions, respectively. Increasing the biodiesel fraction to B5 and B20 prolonged the ignition delay by 48.5 and 50.7 CAD from 47 CAD of the baseline engine;
4. The maximum in-cylinder pressure was reduced by 3% for B5 and 10.2% for B20 in comparison to B0;
5. By increasing the biodiesel fraction, the combustion stability decreased. Using COV IMEP as an indicator of combustion variability, it increased from 1.8% for B0 to 4.2% for B5 and 4.8 for B20. The cyclic variations of IMEP, combustion duration, and start of combustion indicated that the addition of biodiesel to DFI increased the standard deviation and generally made the combustion more unstable;
6. The tendency to knock was decreased by increasing the fraction of biodiesel in DFI. The knocking tendency decreased from 13.7% for the baseline case (B0) to 4.3% for B20;
7. The baseline case (B0) had no misfiring cycle, and the B5 case had some misfiring cycles, but no knocking cycle was observed.
8. This study shows that the addition of sunflower methyl ester as an additive to diesel direct fuel injection leads to more cyclic variations of RCCI combustion under low loads conditions. In other words, it makes combustion more unstable. The use of other biodiesel or biofuels with different physical and chemical properties and investigation of their impacts on combustion characteristics, stability, and engine-out emissions is the subject of future research. Moreover, numerical studies will provide an insightful perspective on the use of various biodiesels in RCCI combustion.

Author Contributions: Conceptualization, M.T.Z. and V.H.; methodology, M.T.Z. and V.H.; formal analysis, M.T.Z. and V.H.; investigation, M.T.Z. and V.H.; resources, V.H.; data curation, M.T.Z.; writing—original draft preparation, M.T.Z.; writing—V.H.; visualization, M.T.Z.; supervision, V.H.; project administration, V.H.; All authors have read and agreed to the published version of the manuscript.

Funding: The authors acknowledge the Simon Fraser University Central Open Access Fund, covering journal fees.

Institutional Review Board Statement: Not Applicable.

Informed Consent Statement: Not Applicable.

Acknowledgments: The contributions and support of FCE research lab staff and grad students, M.H. Hosseinian, M. Reyhanian, and S. Ghaffarzadeh are acknowledged.

Conflicts of Interest: The authors declare no conflict of interest.

Nomenclature

aTDC	After top dead center	IMEP	Indicated mean effective pressure
CA10	Crank angle due to 10% heat release	iTH	Indicated thermal efficiency
CA50	Crank angle due to 50% heat release	LHV	Lower heating value
CA90	Crank angle due to 90% heat release	LTC	Low temperature combustion
CAD	Crank angle degree	NG	Natural gas
CD	Combustion duration	NGEF	Natural gas energy fraction
CO	Carbon monoxide	NOx	Nitrogen oxides
CO_2	Carbon dioxide	PFI	Port fuel injection
COV	Coefficient of variance	PPC	Partially premixed charge
DFI	Direct fuel injection	RCCI	Reactivity controlled compression ignition
H2	Hydrogen	rpm	Revolution per minute
HCCI	Homogeneous charge compression ignition	SOI	Start of injection
HRR	Heat release rate	UHC	Unburned hydrocarbon
ID	Ignition delay		

References

1. Sanjeevannavar, M.B.; Banapurmath, N.R.; Soudagar, M.E.M.; Atgur, V.; Hossain, N.; Mujtaba, M.A.; Yunus Khan, T.M.; Nageswar Rao, B.; Ismail, K.A.; Elfasakhany, A. Performance indicators for the optimal BTE of biodiesels with additives through engine testing by the Taguchi approach. *Chemosphere* **2022**, *288*, 132450. [CrossRef] [PubMed]
2. Tompkins, B.T.; Jacobs, T.J. Low-temperature combustion with biodiesel: Its enabling features in improving efficiency and emissions. *Energy Fuels* **2013**, *27*, 2794–2803. [CrossRef]
3. Zhang, J.J.; Wei, Y.; Fang, Z. Ozone pollution: A major health hazard worldwide. *Front. Immunol.* **2019**, *10*, 2518. [CrossRef] [PubMed]
4. Valavanidis, A.; Vlachogianni, T.; Fiotakis, K.; Loridas, S. Pulmonary oxidative stress, inflammation and cancer: Respirable particulate matter, fibrous dusts and ozone as major causes of lung carcinogenesis through reactive oxygen species mechanisms. *Int. J. Environ. Res. Public Health* **2013**, *10*, 3886–3907. [CrossRef]
5. Kulkarni, P.C. Reducing Green House Effect Caused by Soot via Oxidation Using Modified $LaFe_{1-x}Cu_xO_3$ Catalysts. In *Global Warming and Climate Change*; IntechOpen: London, UK, 2019.
6. Xu, G.; Jia, M.; Li, Y.; Chang, Y.; Wang, T. Potential of reactivity controlled compression ignition (RCCI) combustion coupled with variable valve timing (VVT) strategy for meeting Euro 6 emission regulations and high fuel efficiency in a heavy-duty diesel engine. *Energy Convers. Manag.* **2018**, *171*, 683–698. [CrossRef]
7. Duraisamy, G.; Rangasamy, M.; Ramasankaran, A.P. Statistical and experimental investigation of single fuel reactivity controlled compression ignition combustion on a non-road diesel engine. *Energy Convers. Manag.* **2019**, *199*, 112025. [CrossRef]
8. Benajes, J.; García, A.; Monsalve-Serrano, J.; Villalta, D. Benefits of E85 versus gasoline as low reactivity fuel for an automotive diesel engine operating in reactivity controlled compression ignition combustion mode. *Energy Convers. Manag.* **2018**, *159*, 85–95. [CrossRef]
9. Kousheshi, N.; Yari, M.; Paykani, A.; Saberi Mehr, A.; de la Fuente, G.F. Effect of syngas composition on the combustion and emissions characteristics of a syngas/diesel RCCI engine. *Energies* **2020**, *13*, 212. [CrossRef]
10. Muniappan, K.; Sheshadri, S.; Duvvuri, P.P. Numerical Analysis of the Effects of Direct Dual Fuel Injection on the Compression Ignition Engine. *ACS Omega* **2020**, *5*, 30047–30058. [CrossRef]
11. Wenming, Y.; Meng, Y. Phi-T map analysis on RCCI engine fueled by methanol and biodiesel. *Energy* **2019**, *187*, 115958. [CrossRef]
12. Zheng, Z.; Xia, M.; Liu, H.; Shang, R.; Ma, G.; Yao, M. Experimental study on combustion and emissions of n-butanol/biodiesel under both blended fuel mode and dual fuel RCCI mode. *Fuel* **2018**, *226*, 240–251. [CrossRef]
13. Harari, P.; Banapurmath, N.; Yaliwal, V.; Khan, T.; Badruddin, I.A.; Kamangar, S.; Mahlia, T.M.I. Effect of Injection Timing and Injection Duration of Manifold Injected Fuels in Reactivity Controlled Compression Ignition Engine Operated with Renewable Fuels. *Energies* **2021**, *14*, 4621. [CrossRef]
14. Li, R.; Liu, Z.; Han, Y.; Cai, Y.; Wang, X.; Zheng, J.; Tan, M.; Xu, Y.; Tian, J.; Meng, X. Target-Oriented Fuel Design for the Homogeneous Charge Autoignition Combustion Mode: A Case Study of an-Heptane–PODE3–Ethanol Mixture. 1. A Pathway To Increase the Combustion Efficiency and Reduce Pollutant Emissions. *Energy Fuels* **2018**, *33*, 16–30. [CrossRef]
15. Sun, C.; Kang, D.; Bohac, S.V.; Boehman, A.L. impact of fuel and injection timing on partially premixed charge compression ignition combustion. *Energy Fuels* **2016**, *30*, 4331–4345. [CrossRef]
16. Benajes, J.; García, A.; Monsalve-Serrano, J.; Sari, R.L. Experimental investigation on the efficiency of a diesel oxidation catalyst in a medium-duty multi-cylinder RCCI engine. *Energy Convers. Manag.* **2018**, *176*, 1–10. [CrossRef]
17. Xu, Z.; Jia, M.; Xu, G.; Li, Y.; Zhao, L.; Xu, L.; Lu, X. Potential for reducing emissions in reactivity-controlled compression ignition engines by fueling syngas and diesel. *Energy Fuels* **2018**, *32*, 3869–3882. [CrossRef]

18. Yousefi, A.; Guo, H.; Birouk, M.; Liko, B. On greenhouse gas emissions and thermal efficiency of natural gas/diesel dual-fuel engine at low load conditions: Coupled effect of injector rail pressure and split injection. *Appl. Energy* **2019**, *242*, 216–231. [CrossRef]
19. Yousefi, A.; Guo, H.; Birouk, M. Effect of diesel injection timing on the combustion of natural gas/diesel dual-fuel engine at low-high load and low-high speed conditions. *Fuel* **2019**, *235*, 838–846. [CrossRef]
20. García, A.; Monsalve-Serrano, J.; Roso, V.R.; Martins, M.E.S. Evaluating the emissions and performance of two dual-mode RCCI combustion strategies under the World Harmonized Vehicle Cycle (WHVC). *Energy Convers. Manag.* **2017**, *149*, 263–274. [CrossRef]
21. Karczewski, M.; Chojnowski, J.; Szamrej, G. A Review of Low-CO2 Emission Fuels for a Dual-Fuel RCCI Engine. *Energies* **2021**, *14*, 5067. [CrossRef]
22. Ogunkunle, O.; Ahmed, N.A. A review of global current scenario of biodiesel adoption and combustion in vehicular diesel engines. *Energy Rep.* **2019**, *5*, 1560–1579. [CrossRef]
23. Gashaw, A.; Teshita, A. Production of biodiesel from waste cooking oil and factors affecting its formation: A review. *Int. J. Renew. Sustain. Energy* **2014**, *3*, 92–98.
24. Yaqoob, H.; Teoh, Y.H.; Sher, F.; Farooq, M.U.; Jamil, M.A.; Kausar, Z.; Sabah, N.U.; Shah, M.F.; Rehman, H.Z.U.; Rehman, A.U. Potential of Waste Cooking Oil Biodiesel as Renewable Fuel in Combustion Engines: A Review. *Energies* **2021**, *14*, 2565. [CrossRef]
25. Firoz, S. A review: Advantages and disadvantages of biodiesel. *Int. Res. J. Eng. Technol.* **2017**, *4*, 530–533.
26. Lin, L.; Cunshan, Z.; Vittayapadung, S.; Xiangqian, S.; Mingdong, D. Opportunities and challenges for biodiesel fuel. *Appl. Energy* **2011**, *88*, 1020–1031. [CrossRef]
27. Khan, H.; Soudagar, M.E.M.; Kumar, R.H.; Safaei, M.R.; Farooq, M.; Khidmatgar, A.; Banapurmath, N.R.; Farade, R.A.; Abbas, M.M.; Afzal, A. Effect of nano-graphene oxide and n-butanol fuel additives blended with diesel—Nigella sativa biodiesel fuel emulsion on diesel engine characteristics. *Symmetry* **2020**, *12*, 961. [CrossRef]
28. Soudagar, M.E.M.; Banapurmath, N.; Afzal, A.; Hossain, N.; Abbas, M.M.; Haniffa, M.A.C.M.; Naik, B.; Ahmed, W.; Nizamuddin, S.; Mubarak, N. Study of diesel engine characteristics by adding nanosized zinc oxide and diethyl ether additives in Mahua biodiesel–diesel fuel blend. *Sci. Rep.* **2020**, *10*, 15326. [CrossRef]
29. Jeswani, H.K.; Azapagic, A. Life Cycle Sustainability Assessment of Second Generation Biodiesel. In *Advances in Biodiesel Production*; Elsevier: Amsterdam, The Netherlands, 2012; pp. 13–31.
30. Du, H.; Huque, Z.; Kommalapati, R.R. Impacts of Biodiesel Applied to the Transportation Fleets in the Greater Houston Area. *J. Renew. Energy* **2018**, *2018*, 7350715. [CrossRef]
31. Diesel Vehicles Using Biodiesel. 2018. Available online: https://afdc.energy.gov/vehicles/diesel.html (accessed on 20 December 2021).
32. Charitha, V.; Thirumalini, S.; Prasad, M.; Srihari, S. Investigation on performance and emissions of RCCI dual fuel combustion on diesel-bio diesel in a light duty engine. *Renew. Energy* **2019**, *134*, 1081–1088. [CrossRef]
33. Zheng, Z.; Xia, M.; Liu, H.; Wang, X.; Yao, M. Experimental study on combustion and emissions of dual fuel RCCI mode fueled with biodiesel/n-butanol, biodiesel/2, 5-dimethylfuran and biodiesel/ethanol. *Energy* **2018**, *148*, 824–838. [CrossRef]
34. Thomas, J.J.; Sabu, V.; Nagarajan, G.; Kumar, S.; Basrin, G. Influence of waste vegetable oil biodiesel and hexanol on a reactivity controlled compression ignition engine combustion and emissions. *Energy* **2020**, *206*, 118199. [CrossRef]
35. Benajes, J.; García, A.; Monsalve-Serrano, J.; Balloul, I.; Pradel, G. An assessment of the dual-mode reactivity controlled compression ignition/conventional diesel combustion capabilities in a EURO VI medium-duty diesel engine fueled with an intermediate ethanol-gasoline blend and biodiesel. *Energy Convers. Manag.* **2016**, *123*, 381–391. [CrossRef]
36. Agarwal, A.K.; Singh, A.P.; Maurya, R.K. Evolution, challenges and path forward for low temperature combustion engines. *Prog. Energy Combust. Sci.* **2017**, *61*, 1–56. [CrossRef]
37. Ansari, E.; Menucci, T.; Shahbakhti, M.; Naber, J. Experimental investigation into effects of high reactive fuel on combustion and emission characteristics of the Diesel-Natural gas Reactivity Controlled Compression Ignition engine. *Appl. Energy* **2019**, *239*, 948–956. [CrossRef]
38. Kakoee, A.; Bakhshan, Y.; Aval, S.M.; Gharehghani, A. An improvement of a lean burning condition of natural gas/diesel RCCI engine with a pre-chamber by using hydrogen. *Energy Convers. Manag.* **2018**, *166*, 489–499. [CrossRef]
39. Kalsi, S.S.; Subramanian, K. Experimental investigations of effects of hydrogen blended CNG on performance, combustion and emissions characteristics of a biodiesel fueled reactivity controlled compression ignition engine (RCCI). *Int. J. Hydrog. Energy* **2017**, *42*, 4548–4560. [CrossRef]
40. Harari, P.; Banapurmath, N.; Yaliwal, V.; Khan, T.Y.; Soudagar, M.E.M.; Sajjan, A. Experimental studies on performance and emission characteristics of reactivity controlled compression ignition (RCCI) engine operated with gasoline and Thevetia Peruviana biodiesel. *Renew. Energy* **2020**, *160*, 865–875. [CrossRef]
41. Işik, M.Z.; Aydin, H. Investigation on the effects of gasoline reactivity controlled compression ignition application in a diesel generator in high loads using safflower biodiesel blends. *Renew. Energy* **2019**, *133*, 177–189. [CrossRef]
42. Giakoumis, E.G.; Sarakatsanis, C.K. Estimation of biodiesel cetane number, density, kinematic viscosity and heating values from its fatty acid weight composition. *Fuel* **2018**, *222*, 574–585. [CrossRef]
43. Duan, H.; Jia, M.; Chang, Y.; Liu, H. Experimental study on the influence of low-temperature combustion (LTC) mode and fuel properties on cyclic variations in a compression-ignition engine. *Fuel* **2019**, *256*, 115907. [CrossRef]

44. Saxena, M.R.; Maurya, R.K. *Effect of Diesel Injection Timing on Peak Pressure Rise Rate and Combustion Stability in RCCI Engine*; SAE Technical Paper; SAE International: Warrendale, PA, USA, 2018.
45. Klos, D.T.; Kokjohn, S.L. Investigation of the effect of injection and control strategies on combustion instability in reactivity-controlled compression ignition engines. *J. Eng. Gas Turbines Power* **2016**, *138*, 011502. [CrossRef]
46. Saxena, M.R.; Maurya, R.K. *Experimental Investigation of Combustion Stability and Particle Emission from CNG/Diesel RCCI Engine*; SAE Technical Paper; SAE International: Warrendale, PA, USA, 2020.
47. Tripathi, G.; Sharma, P.; Dhar, A. Effect of methane augmentation on combustion stability and unregulated emissions in compression ignition engine. *Fuel* **2020**, *263*, 116672. [CrossRef]
48. Duraisamy, G.; Rangasamy, M.; Nagarajan, G. *Effect of EGR and Premixed Mass Percentage on Cycle to Cycle Variation of Methanol/Diesel Dual Fuel RCCI Combustion*; SAE Technical Paper; SAE International: Warrendale, PA, USA, 2019.
49. Ghaffarzadeh, S.; Toosi, A.N.; Hosseini, V. An experimental study on low temperature combustion in a light duty engine fueled with diesel/CNG and biodiesel/CNG. *Fuel* **2020**, *262*, 116495. [CrossRef]
50. Noor, C.W.M.; Mamat, R.; Ali, O.; Najafi, G.; Mansor, W.N.D. Cyclic Variation Analysis of Palm Biodiesel Fuel in Low Compression Marine Diesel Engine. *J. Adv. Res. Fluid Mech. Therm. Sci.* **2020**, *75*, 43–58. [CrossRef]
51. Santos, B.S.; Capareda, S.C.; Capunitan, J.A. Sunflower methyl ester as an engine fuel: Performance evaluation and emissions analysis. *Int. Sch. Res. Not.* **2013**, *2013*, 352024. [CrossRef]
52. Hussain, F.; Soudagar ME, M.; Afzal, A.; Mujtaba, M.A.; Fattah, I.M.; Naik, B.; Mulla, M.H.; Badruddin, I.A.; Yunus Khan, T.M.; Raju, V.D.; et al. Enhancement in Combustion, Performance, and Emission Characteristics of a Diesel Engine Fueled with Ce-ZnO Nanoparticle Additive Added to Soybean Biodiesel Blends. *Energies* **2020**, *13*, 4578. [CrossRef]
53. Ra, Y.; Reitz, R.D.; McFarlane, J.; Daw, C.S. Effects of fuel physical properties on diesel engine combustion using diesel and bio-diesel fuels. *SAE Int. J. Fuels Lubr.* **2009**, *1*, 703–718. [CrossRef]
54. European Emission Standards. Available online: https://dieselnet.com/standards/eu/hd.php#stds (accessed on 20 December 2021).
55. Wategave, S.; Banapurmath, N.; Sawant, M.; Soudagar, M.E.M.; Mujtaba, M.; Afzal, A.; Basha, J.S.; Alazwari, M.A.; Safaei, M.R.; Elfasakhany, A. Clean combustion and emissions strategy using reactivity controlled compression ignition (RCCI) mode engine powered with CNG-Karanja biodiesel. *J. Taiwan Inst. Chem. Eng.* **2021**, *124*, 116–131. [CrossRef]
56. Reitz, R.D.; Duraisamy, G. Review of high efficiency and clean reactivity controlled compression ignition (RCCI) combustion in internal combustion engines. *Prog. Energy Combust. Sci.* **2015**, *46*, 12–71. [CrossRef]
57. Singh, A.P.; Kumar, V.; Agarwal, A.K. Evaluation of comparative engine combustion, performance and emission characteristics of low temperature combustion (PCCI and RCCI) modes. *Appl. Energy* **2020**, *278*, 115644. [CrossRef]
58. Uyumaz, A. An experimental investigation into combustion and performance characteristics of an HCCI gasoline engine fueled with n-heptane, isopropanol and n-butanol fuel blends at different inlet air temperatures. *Energy Convers. Manag.* **2015**, *98*, 199–207. [CrossRef]
59. Valladolid, P.G.; Tunestål, P.; Monsalve-Serrano, J.; García, A.; Hyvönen, J. impact of diesel pilot distribution on the ignition process of a dual fuel medium speed marine engine. *Energy Convers. Manag.* **2017**, *149*, 192–205. [CrossRef]
60. Bahri, B.; Aziz, A.A.; Shahbakhti, M.; Said, M.F.M. Understanding and detecting misfire in an HCCI engine fuelled with ethanol. *Appl. Energy* **2013**, *108*, 24–33. [CrossRef]